Homogeneity of Graphite-Monochromated X-ray Beams

By A. Katrusiak

Department of Chemistry, Adam Mickiewicz University, Grunwaldzka 6, 60-780 Poznań, Poland

and T. W. Ryan

Department of Physics, University of Edinburgh, King's Buildings, Mayfield Road, Edinburgh EH9 3JZ, Scotland

Abstract

The factors influencing the homogeneity of the incident X-ray beam when a graphite monochromator is applied are discussed, in particular the influence of the size and shape of the focal spot of the X-ray tube and the diffraction angle of the monochromator. Beam profiles have been measured for several commonly used X-ray tubes – with a fine or normal focus – and compared. It is shown that in certain cases the normal-focus X-ray tubes give a much broader high-intensity region of the incident beam than the fine-focus X-ray tubes.

Introduction

Homogeneity of the incident beam is one of the most important factors in any X-ray diffraction experiments involving reflection-intensity measurements. It was shown that the distribution of intensity within the incident beam can be seriously affected when a monochromator is used (Coppens, Ross, Blessing, Cooper, Larsen, Leipoldt & Rees, 1974) and a correction procedure for the errors in single-crystal intensities due to the inhomogeneity of the incident beam has been developed and tested by Harkema, Dam, van Hummel & Reuvers (1980). The principal reason proposed to explain the inhomogeneity of the monochromated beam is the low monochromator diffraction angle. Therefore, this problem is especially acute for the shorter X-ray wavelengths, Mo $K\alpha$ and Ag $K\alpha$. When using Mo or Ag X-ray tubes some authors prefer to use β-filters rather than a monochromator (Coppens, Ross, Blessing, Cooper, Larsen, Leipoldt & Rees, 1974). The problem of inhomogeneity is believed to be less severe or even absent for Cu $K\alpha$ radiation (Birknes & Hansen, 1983).

When a β-filter is used the size and homogeneity of the X-ray beam are entirely controlled by the choice of the primary-beam collimator. For this arrangement the optimum X-ray source is the small brilliant focal spot of a fine-focus X-ray tube. Fine-focus X-ray tubes are also commonly used and, indeed, are recom-

mended for use in diffractometers equipped with graphite monochromators.

In this paper we shall examine the significance of the X-ray tube source size and of the monochromator arrangement on the homogeneity of the primary X-ray beam when a graphite monochromator is used. In the discussion, an elementary background to the *modus operandi* of mosaic monochromator crystals is presented to explain the results of our measurements.

Theoretical background

The pyrolytic graphite monochromator crystals commonly in use in X-ray diffraction equipment are usually Union Carbide grade ZYA, with a mosaic spread [full width at half maximum (FWHM)] of $0{\cdot}4$ (1)°. The 00.2 reflection is normally used ($d_{00.2} = 3{\cdot}355$ Å). For the commonly used X-ray spectral lines Cu $K\alpha$, Mo $K\alpha$ and Ag $K\alpha$ the monochromator Bragg angles are $13{\cdot}3$, $6{\cdot}1$ and $4{\cdot}7°$, respectively. Pyrolytic graphite monochromators, like any other highly mosaic crystals, are composed of a large number of mosaic blocks (Kan, Misenheimer, Forster & Moss, 1987). The mutual misalignment of these mosaic blocks about the [00.*l*] axis is described by a Gaussian distribution with a FWHM of about $0{\cdot}4°$. Fig. 1 shows a schematic ray diagram illustrating diffraction of monochromatic X-rays from a point source S by a mosaic crystal. For a symmetrically cut
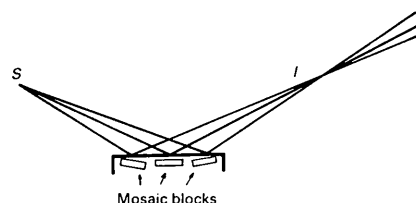

Fig. 1. Schematic ray diagram illustrating the diffraction of monochromatic X-rays from a point source (S) by a mosaic crystal (pyrolytic graphite). Size of the mosaic blocks, their misalignment and divergence of the beam are enhanced for clarity – the misalignment and divergence are about $0{\cdot}4°$ for pyrolitic graphite.

© 1988 International Union of Crystallography

monochromator crystal (i.e. when the scattering vector is normal to the crystal face) a focused image of the source S convoluted with the distribution function of the mosaic spread in the monochromator is produced at point I and the source–monochromator distance is equal to the distance from the monochromator to the image I. Several other X-ray optical factors affect the spatial distribution of the intensity of the diffracted X-ray beam at I (Mathieson, 1985). They include the penetration of X-rays into the crystal (i.e. the beam is not diffracted only from the surface), absorption and extinction of the X-ray beams within the monochromator crystal; but these effects are of secondary importance in the context of the present discussion.

For a polychromatic source (i.e. a normal X-ray tube producing a $K\alpha_1\alpha_2$ doublet and $K\beta$ lines superimposed upon a *Bremsstrahlung* background) the mosaic monochromator produces a series of spectrally dispersed images of the source S at $I_{\alpha1}$, $I_{\alpha2}$ and I_β respectively, as shown in Fig. 2.

The role of the primary-beam collimator in X-ray diffractometers equipped with a graphite monochromator is different in the vertical and horizontal directions normal to the direction of the collimator (see Fig. 3). The preceding arguments show that the collimation in direction $v^i_\perp$ coplanar with $[00.l]$ (i.e. vertical direction z on CAD-4 or Seimens diffractometers and the horizontal y direction on Syntex $P2_1$ or Rigaku diffractometers) is governed by the source size and the focusing properties of the monochromator crystal. The collimator serves to eliminate the $K\beta$ component and to reduce the amount of transmitted white radiation, but collimates the $K\alpha$ primary beam only in direction $v_\parallel$ normal to the beam and to $[00.l]$ of the monochromator.
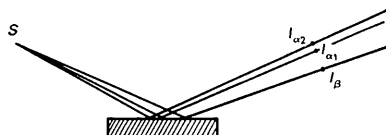

Fig. 2. Schematic ray diagram of the polychromatic X-ray beam reflected from the monochromator crystal.
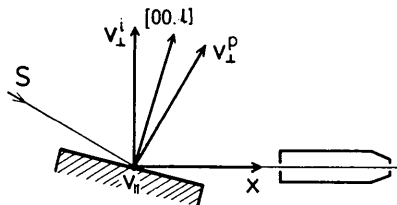

Fig. 3. Monochromator–collimator arrangement and vector definitions: x along the reflected beam, $v_\parallel$ coplanar with the reflecting monochromator plane and normal to x, $v^p_\perp$ normal to x and to $v_\parallel$, $v^i_\perp$ normal to the beam from the source and to $v_\parallel$.

Two main monochromator arrangements applied in the most common X-ray four-circle diffractometers are schematically presented in Fig. 4: (a) In the so-called 'perpendicular' geometry (Fig. 4a) the scattering plane of the monochromator is perpendicular to the scattering plane of the sample crystal (i.e. to the horizontal xy plane of the diffractometer); the 'perpendicular' geometry is applied in such diffractometers as CAD-4, Siemens and most Syntex $P1$'s. (b) The so-called 'parallel' geometry (Fig. 4b) has the scattering plane of the monochromator coplanar with the scattering plane of the sample crystal (the diffractometer xy plane) – this geometry is incorporated on diffractometers like Syntex $P2_1$ or Rigaku.

However, the position of the X-ray tube with respect to the monochromator crystal and to the diffractometer is not described unequivocally by the above definitions. Fig. 4 shows the position of the X-ray tube as it is mounted by the leading manufacturers of X-ray diffractometers. For both 'perpendicular' and 'parallel' geometries the X-ray tube is positioned horizontally. A vertical position for the X-ray tube is also possible and equally effective. As the position of the X-ray tube with respect to the monochromator crystal is a vital point in the further argument, let us incorporate this information into the definition of monochromator geometry.* There are four cases:

(a) horizontal X-ray tube and 'perpendicular' monochromator geometry (H/PE) – Fig. 4(a);

(b) horizontal X-ray tube and 'parallel' monochromator (H/PA) – Fig. 4(b);

(c) vertical X-ray tube and 'perpendicular' monochromator (V/PE);

(d) vertical X-ray tube and 'parallel' monochromator (V/PA).

Thus, geometries H/PE and V/PE (or H/PA and V/PA) will have the same polarization corrections for the intensity measurements of the sample-crystal reflections, while the same X-ray tube/monochromator-crystal arrangements are in the H/PE and V/PA geometries or in the V/PE and H/PA geometries.

The X-ray tubes commonly used on single-crystal diffractometers have linear anodes, the dimensions of which are given in Table 1 (Philips, 1985). The point-focus window is used when viewing the linear anode from the end at a small take-off angle – usually about 6° (see Fig. 4) – so the line image is foreshortened and appears as a rectangle, the dimensions of which, depending on the anode dimensions, are also given in Table 1.

---

* One can consider the vertical position of the X-ray tube by interchanging 'horizontal views' with 'views from above' in Fig. 4. Consequently, the 'perpendicular' and 'parallel' modes will have to be exchanged as well.

Table 1. *Focus types of the most commonly used X-ray tubes, the focus dimensions of their anodes and the focal dimensions at 6° take-off angle* (*Philips*, 1985)

These are standard values also applied by other X-ray tube manufacturers.

Focus type	Focus dimensions (mm)	Focal dimensions at 6° take-off angle: point focus (mm)
Fine	0·4×8·0	0·4×0·8
Long fine	0·4×12·0	0·4×1·2
Normal	1·0×10·0	1·0×1·0
Broad	2·0×12·0	2·0×1·2

Table 2. *Focal dimension along* $v_\perp^p$ *for various focus types and X-ray tube/monochromator arrangements*

Focus type	Focal dimension along $v_\perp^p$ at 6° take-off angle (point focus) (mm)			
	H/PE	H/PA	V/PE	V/PA
Fine	0·4	0·8	0·8	0·4
Long fine	0·4	1·2	1·2	0·4
Normal	1·0	1·0	1·0	1·0
Broad	2·0	1·2	1·2	2·0

As stated previously, the X-ray source size in the direction parallel to the reflecting plane of the monochromator and normal to the beams ($v_\parallel$ – see Fig. 3) has no effect on the width and homogeneity of the reflected beam in this direction. The width is controlled by the collimator and the beam is homogeneous along $v_\parallel$. The size of the X-ray source in the direction of $v_\perp^p$ is reflected in the image produced by the scattered radiation (Fig. 1). Thus, the dimension of the point focus in this direction has a significant effect on the homogeneity of the beam along $v_\perp^i$ (see diagrams in Fig. 4). Consequently, the longer the view of the X-ray source along $v_\perp^p$, the broader is the image of the source produced along $v_\perp^i$.

Inspection of the values in Table 1 brings us to the main point of the discussion. Table 2 gives the focal dimension along $v_\perp^p$ depending on the focus type and the X-ray tube/monochromator arrangement. It can be seen that for H/PA geometry there is little difference in the focal dimension along $v_\perp^p$ between the most commonly used fine- and normal-focus X-ray tubes. However, this dimension is much shorter

for the H/PE mode when a fine-focus X-ray tube is used.

Experimental

The measurements of the beam-intensity distribution have been performed on a Syntex $P2_1$ and two CAD-4 diffractometers. A pinhole 0·025 mm in diameter in a gold foil was used. After ensuring the good centring of the primary X-ray beam, the pinhole was centred in the sample-crystal position of the diffractometer. The pinhole was mounted on a goniometer head perpendicular to the beam. The distribution of the intensity within the beam was measured with a stationary detector. No apertures were used, only aluminum foil as an attenuator to protect the detector. The pinhole was displaced from the centre along $v_\perp^i$ (*i.e.* the pinhole was displaced vertically on the CAD-4 and horizontally on the Syntex $P2_1$) using the transmission of the goniometer head, in 25 or 50 μm steps. A short collimator, 2·5 mm in diameter, was used. Graphite-monochromated X-ray beams of Mo and Cu X-ray tubes with fine focus (FF) and with normal focus (NF) were tested.
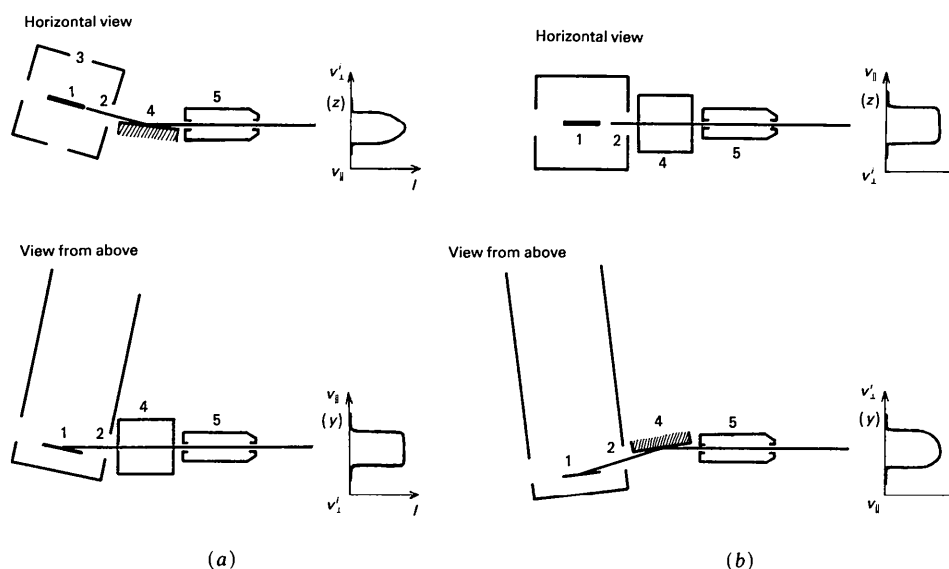

Fig. 4. (a) 'Perpendicular' and (b) 'parallel' geometries of the monochromator: (1) linear focus; (2) point-focus Be window; (3) line-focus Be window; (4) monochromator crystal; (5) collimator.

Results and discussion

Fig. 5 presents the intensity distribution across the primary X-ray beam, along $v_\perp^i$, on a CAD-4 diffractometer (H/PE – vertical displacements of the pinhole) measured in the following cases:

(a) graphite-monochromated Mo $K\alpha$ X-ray beam, 00.2 reflection, FF X-ray tube;

(b) graphite-monochromated Mo $K\alpha$ beam, 00.2 reflection, FF X-ray tube; another CAD-4 diffractometer;

(c) graphite-monochromated Mo $K\alpha$ beam, 00.4 reflection, FF X-ray tube;

(d) graphite-monochromated Mo $K\alpha$ beam, 00.2 reflection, NN X-ray tube.

All these profiles of the primary beams are bell-shaped. The first two plots are very similar as they were obtained with the same type of X-ray tube and the same monochromator geometry but with two different CAD-4 diffractometers to check the repeatability of our measurements – one of the primary beams (a) is only insignificantly broader than the other. Plot (c) was obtained in the same conditions as plot (a) but reflection 00.4 was used and the monochromator angle was increased to $\theta(00.4) = 12\cdot2°$ [this value approximates $\theta(00.2) = 13\cdot3°$ for Cu $K\alpha$]. Thus, comparison of plot (a) or (b) with plot (c) illustrates the influence of the monochromator angle on the width of the beam profile. Plot (d) was obtained in the same conditions as plot (a) but a NF X-ray tube was used – it shows how significantly the width of the beam profile is influenced by the size of the focal spot of the X-ray tube.

Fig. 6 shows two profiles of graphite-monochromated X-ray beams measured on a Syntex $P2_1$ diffractometer (H/PA). In this plot the x axis represents the horizontal displacement of the pinhole from the beam centre. The two cases are

(e) graphite-monochromated Mo $K\alpha$ beam, 00.2 reflection, NF X-ray tube;

(f) graphite-monochromated Cu $K\alpha$ beam, 00.2 reflection, NF X-ray tube.

Profile (f) is broader than profile (e), which shows the influence of the monochromator angle to be more than twice as large for Cu $K\alpha$ (f) than for Mo $K\alpha$ (e). Profile (d) (Fig. 5) and profile (e) have the same width which follows the same monochromator angle and the same focal dimension of the X-ray source along $v_\perp^p$ (vertical on the CAD-4 and horizontal on the Syntex $P2_1$) in both these measurements (see Table 2). All the profiles are bell-shaped and they have no plateau area. The beam region with intensity over 90% differs very significantly for the beam profiles presented above and is less than 0·25 mm for plot (a) or (b), about 0·40 mm for plot (d) or (e) and 0·60 mm for plot (f). Scans across the beams along $v_\parallel$ were also done (horizontal on the CAD-4 and vertical on the Syntex $P2_1$) and showed plateaux limited by the collimator. Differences in intensity up to about 4% were noted within the plateau regions.

The above results can be summarized as follows:

(1) For the H/PE (or V/PA) monochromator geometry, NF X-ray tubes are recommended for use on diffractometers, as they give a much broader high-intensity region of the primary beam along $v_\perp^i$ than the FF X-ray tubes.
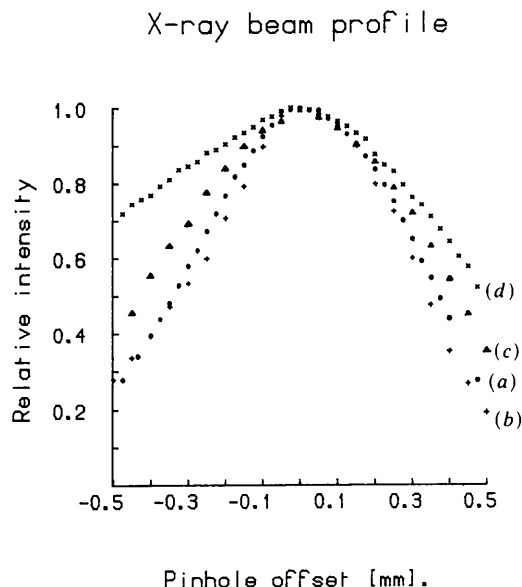

Fig. 5. Beam-intensity profiles measured on CAD-4 diffractometers along z in the following conditions: (a) FF Mo X-ray tube, 00.2 monochromator reflection; (b) as (a), but another CAD-4; (c) as (a), but 00.4 monochromator reflection; (d) as (a) but a NF X-ray tube was used.
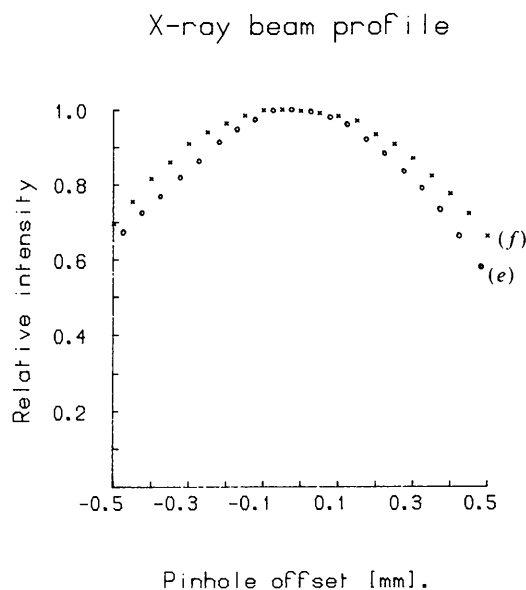

Fig. 6. Beam-intensity profiles measured on a Syntex $P2_1$ diffractometer along y: (e) Mo $K\alpha$ beam, NF X-ray tube, 00.2 monochromator reflection; (f) as (e) but Cu $K\alpha$ beam.

(2) The FF X-ray tubes are recommended for the diffractometers with monochromator geometry H/PA (or V/PE), as, in this case, the homogeneity of the monochromated beam is not influenced by the width of the X-ray tube focus.

(3) All the graphite-monochromated X-ray beams, including the Cu $K\alpha$ one, have a bell-shaped profile along $v'_\perp$ and a plateau along $v_\parallel$.

The quality of the primary beam should be taken into consideration when preparing a sample crystal for data collection (Tanaka, 1978). For Mo $K\alpha$ FF tube and H/PE geometry the 90% region of the beam is less than 0·25 mm and drops steeply outside this range, which introduces the possibility of serious systematic errors. Large and irregular-shaped crystals are especially objectionable as the volume of such a crystal contained within the high-intensity region changes significantly when the crystal is reoriented for different diffractometer settings. Unfortunately, large platelets or needle-shaped samples, longer than 0·5 or even 0·7 mm, are occasionally used when Mo $K\alpha$ FF X-ray tubes and H/PE monochromator geometry are applied.

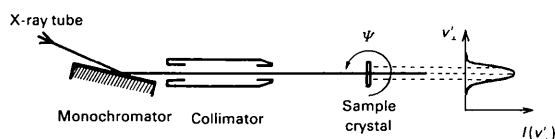The intensity data measured for large irregular-shaped crystals are often corrected for absorption and often Furnas's method based on reflection intensity measurements at different Ψ settings is applied (North, Phillips & Mathews, 1968). It can be seen from Fig. 7 that the rotation of the crystal about the Ψ axis will cause systematic errors due to inhomogeneities of the beam (besides those of absorption) which, when this 'correction' is applied, will add new systematic errors to all the data already affected by the inhomogeneity effect during the data collection. It should be ensured that the sample crystal is small enough to avoid this kind of errors. There are no such errors in Ψ-scanned reflection intensities for H/PA (or V/PE) geometry, as the beam is homogeneous along z for this geometry.

Fig. 7. A platelet sample crystal positioned for a Ψ scan on a diffractometer with H/PE geometry.

References

BIRKNES, B. & HANSEN, L. K. (1983). *J. Appl. Cryst.* **16**, 11–13.
COPPENS, P., ROSS, F. K., BLESSING, R. H., COOPER, W. F., LARSEN, F. K., LEIPOLDT, J. G. & REES, B. (1974). *J. Appl. Cryst.* **7**, 315–319.
HARKEMA, S., DAM, J., VAN HUMMEL, G. J. & REUVERS, A. J. (1980). *Acta Cryst.* **A36**, 433–435.
KAN, X. B., MISENHEIMER, M. E., FORSTER, K. & MOSS, S. C. (1987). *Acta Cryst.* **A43**, 418–425.
MATHIESON, A. McL. (1985). *Acta Cryst.* **A41**, 309–316.
NORTH, A. C. T., PHILLIPS, D. C. & MATHEWS, F. S. (1968). *Acta Cryst.* **A24**, 351–359.
Philips (1985). *X-ray Tubes for Diffraction and Spectrometry.* Philips, The Netherlands.
TANAKA, K. (1978). *Acta Cryst.* **B34**, 2487–2494.

Crystallography, Geometry and Physics in Higher Dimensions. IV. Crystallographic Cells and Polytopes or 'Molecules' of Four-Dimensional Space $\mathbb{E}^4$

BY T. PHAN, R. VEYSSEYRE AND D. WEIGEL

Laboratoire de Chimie-Physique du Solide (Unité associée au CNRS no. 453) et Laboratoire de Mathématiques de la Physique, Ecole Centrale des Arts et Manufactures, Grande Voie des Vignes, 92295 Châtenay-Malabry CEDEX, France

Abstract

In a recent paper [Weigel, Phan & Veysseyre (1987). *Acta Cryst.* A43, 294–304] the 'WPV' notation was proposed for the crystallographic point symmetry groups (PSGs) in four-dimensional space $\mathbb{E}^4$. The geometry of crystal families, systems and cells of $\mathbb{E}^4$ is illustrated with a few geometrical examples of crystallographic point symmetry operations (PSOs). The cells of the 33 crystal systems in $\mathbb{E}^4$ are described and various polytopes are analysed. Some examples of geometry in higher dimensions are explained.